Veering of Rayleigh-Lamb waves in orthorhombic materials

Journal Title
XX(X):2–26

Reprints and permission:
sagepub.co.uk/journalsPermissions.nav
DOI: 10.1177/ToBeAssigned
www.sagepub.com/
SAGE

A. Nobili[1], B. Erbas[2] and C. Signorini[3]

Abstract

We analyse veering of Rayleigh-Lamb waves in a thin orthotropic plate. We demonstrate that veering results from interference of partial waves in a similar manner as it occurs in systems composed of 1D structures, such as beams or strings. Indeed, in the neighbourhood of a veering point, the system may be approximated by a pair of interacting tout strings whose wave speed is the geometric average of the phase and group velocity of the relevant partial wave at the veering point. This complementary pair of partial waves provides the coupling terms in a form compatible with a action-reaction principle. We prove that veering of symmetric waves near the longitudinal bulk wave speed repeats itself indefinitely with the same structure. However, the dispersion behaviour of Rayleigh-Lamb waves is richer than that of 1D systems and this reflects also on the veering pattern. In fact, the interacting tout string model fails whenever the dispersion branch is not guided by either partial wave. This often occurs when neighbouring veering points interact and partial waves no longer provide guiding curves.

Keywords

Veering, Rayleigh-Lamb waves, Orthorhombic elastic materials

Introduction

Rayleigh-Lamb (RL) waves in thin plates have long attracted great attention in view of their theoretical and practical importance. They encompass a large array of important phenomena such as dispersion, localization and interference. Despite their apparent simplicity, a satisfactory understanding of the underlying physics has only been gained in fairly recent times [4]. This understanding is especially valuable because it provides, among many assets, the foundation for consistent asymptotic reduced theories for shell, plates and beams [8, 14, 19, 11]. Consideration of anisotropic features adds considerable complications and yet it possesses relevant practical importance, as well illustrated in the classical monograph [2]. As an example of such complications, following [20] we mention that Kirchhoff-Love and Timoshenko-Reissner plate models fail to be consistent with the outcomes of the 3D theory for a strongly orthotropic material. The recent review paper [9] accounts for the many contributions appearing in the literature that investigate specific features of RL propagation. For example, in [5] it is pointed out that orthotropy is attached to special points possessing zero-group velocity, which pave the way to anomalous dispersion, i.e. situations where the energy flows in the direction opposite to that of propagation for the wave train. Equally, [21] illustrate the effect of curvature on the waveguide properties.

Wave coupling occurs in multiple instances, such as in reduced models, e.g. strings, beams and rods [18, 7] or between different propagation modes, as it is the case for torsional and bending waves [3]. Coupling of waves takes up many different forms (for instance through mode conversion and localization [13]), among which veering is especially remarkable, because it is associated with rapid divergence of the propagation branches in the neighbourhood of the veering point, alongside eigenvector inversion. This peculiar behaviour may be most easily explained in coupled oscillators, where tuning the coupling device brings the specific propagation features of either in a veering condition. In [10, 1],

[1] University of Modena and Reggio Emilia, Department of Engineering Enzo Ferrari, via Vivarelli 10, 41125 Modena, Italy
[2] Eskisehir Technical University, Department of Mathematics, Yunus Emre Campus, 26470, Eskisehir, Turkey
[3] Technical University Dresden, Institute of Construction Materials, Georg-Schumann-Str. 7, 01187 Dresden, Germany

Corresponding author:
Andrea Nobili, Department of Engineering Enzo Ferrari, via Vivarelli 10, 41125 Modena, Italy
Email: andrea.nobili@unimore.it

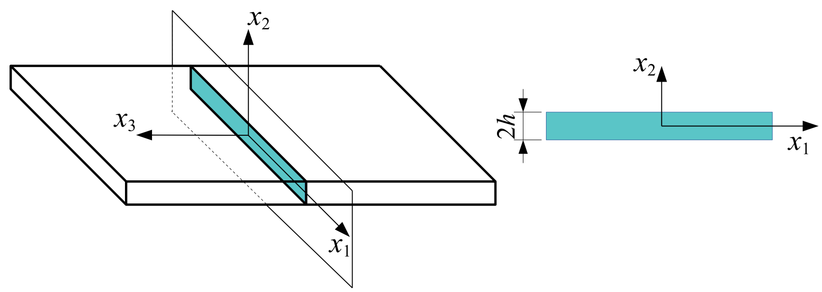

Figure 1. A free infinite orthotropic thin plate in plane strain

Manconi and Mace study veering in discrete conservative elastic systems under a framework for the analysis thereof. They distinguish between weak and strong coupling and introduce the concept of uncoupled block system.

In this paper, we investigate veering in a continuous system, namely for RL waves. In this situation, matter is complicated by the presence of multiple wave modes (branches) and internal coupling. Nonetheless, we can show that the concept of partial waves still work as a building block for both the dispersion pattern and the interference thereof. After developing the classical governing equations and travelling wave solution for orthorhombic media, respectively in Sec. and , partial waves are introduced and analysed in Sec.. In Sec., they are shown to guide RL modes and their intersection defines the veering points and the form of the interacting systems (Sec.). Finally, conclusions are drawn in Sec..

Governing equations

Let us consider an infinite thin plate of thickness $2h$, made of linear elastic homogeneous material with orthorhombic material symmetry (Fig.1). The strip lower/upper boundaries are located, respectively, at $x_2 = \pm h$. We consider the situation when x_3 is a direct axis of even order (i.e. the plane (x_1, x_2) is a mirror plane) and x_1 is directed along a symmetry axis for the material, as in [15]. For convenience, Voigt's (or matrix) notation is adopted throughout [16, p.134], according to which

$$(11) \leftrightarrow 1, (22) \leftrightarrow 2, (33) \leftrightarrow 3, (23) = (32) \leftrightarrow 4, (13) = (31) \leftrightarrow 5, (12) = (21) \leftrightarrow 6.$$

Therefore, as an example, $c_{11} = c_{1111}$, $c_{12} = c_{1122} = c_{2211}$ and $c_{66} = c_{1212} = c_{2112} = c_{2121} = c_{1221}$. The elastic constants are gathered in the stiffness matrix [15, Eq.(3.64)]

$$\mathbf{C} = \begin{bmatrix} c_{11} & c_{12} & c_{13} & 0 & 0 & 0 \\ c_{12} & c_{22} & c_{23} & 0 & 0 & 0 \\ c_{13} & c_{23} & c_{33} & 0 & 0 & 0 \\ 0 & 0 & 0 & c_{44} & 0 & 0 \\ 0 & 0 & 0 & 0 & c_{55} & 0 \\ 0 & 0 & 0 & 0 & 0 & c_{66} \end{bmatrix}. \tag{1}$$

It is important to emphasize that $\mathbf{C}$ is not a rank-2 tensor, for it lacks the transformation property thereof. The off-diagonal coefficients c_{12}, c_{13} and c_{23} are sometimes referred to as coupling stiffnesses and they may be positive, negative or zero. Cubic symmetry, that is considered in [17], may be retrieved upon taking $c_{12} = c_{13} = c_{23}$, $c_{11} = c_{22} = c_{33}$ and $c_{44} = c_{55} = c_{66}$. Isotropic materials are a special case of cubic symmetry with

$$c_{11} = \lambda + 2\mu, \quad c_{12} = \lambda, \quad c_{66} = \mu, \tag{2}$$

where $\mu > 0$ and $\lambda > -\frac{2}{3}\mu$ are Lamé elastic constants. The plane (x_1, x_2) is named the *sagittal plane of wave propagation*, because it contains the surface normal and the propagation direction (wave vector) [16, §5.1]. Under such conditions, it is well known that the Christoffel matrix governing wave propagation has block form and the corresponding linear system breaks up into two independent subsystems: one accounting for longitudinal (P) and shear vertical (SV) propagation (for such motions the polarization vector lies in the sagittal plane) and the other for shear horizontal (SH) propagation, see [16, §5.1.1(a)] and [17]. We recall that positiveness of the strain energy density demands

$$c_{11}, c_{22}, c_{66} > 0, \quad c_{11}c_{22} - c_{12}^2 > 0, \tag{3}$$

so thus we may define the generalized Young modulus

$$E_c = c_{11} - \frac{c_{12}^2}{c_{22}}.$$

It should be emphasized that E_c may be written in terms of the technical (or engineering) moduli [6]

$$E_c = \frac{E_1}{1 - \nu_{13}\nu_{31}},$$

and, in an isotropic material, it reduces to the Young modulus in plane strain $E_c = E/(1-\nu^2)$. We note that, in an anisotropic plate, the bending stiffness within the Kirchhoff theory is given by $D_x = E_c I$ and $D_y = \nu_{31} D_x/\nu_{13}$, wherein $I = 2h^3/3$ is the second moment of inertia, see, for example, [14].

In an orthorhombic material, several bulk wave speeds are defined, see [16],

$$c_1 = \sqrt{\frac{c_{11}}{\rho}}, \quad c_2 = \sqrt{\frac{c_{22}}{\rho}}, \quad c_{SV} = \sqrt{\frac{c_{66}}{\rho}}, \quad c_{SH} = \sqrt{\frac{c_{55}}{\rho}}, \tag{4}$$

respectively bulk longitudinal along x_1 and along x_2 and transverse shear vertical (SV) and shear horizontal (SH) wave speed. To such speeds, in analogy to the longitudinal wave speed for beams, we add the combination [12]

$$c_c = \sqrt{\frac{E_c}{\rho}} < c_1. \tag{5}$$

Strain $\boldsymbol{\epsilon}$ is small and it is related to the displacement field $\boldsymbol{u} = [u_1, u_2, u_3]$ through the linear relations

$$\epsilon_{ij} = \tfrac{1}{2}(u_{i,j} + u_{j,i}), \quad i, j \in \{1, 2, 3\},$$

where a suffix comma denotes differentiation with respect to the relevant space variable, e.g. $u_{1,1} = \partial u_1/\partial x_1$, and summation over twice repeated subscripts is assumed. We recall that $\gamma_{ij} = 2\epsilon_{ij}, i \neq j$ is the engineering shear strain. The stress $\boldsymbol{\sigma}$ is related to strain through Hook's constitutive law

$$\boldsymbol{\sigma} = \mathbf{C}\boldsymbol{\epsilon}. \tag{6}$$

The equilibrium equations, in the absence of body forces, read

$$\sigma_{ij,j} = \rho \ddot{u}_i,$$

and they take on the expanded form (superposed dots denote time differentiation) valid for orthorhombic materials

$$c_{11}u_{1,11} + c_{55}u_{1,33} + c_{66}u_{1,22} + (c_{12}+c_{66})u_{2,12} + (c_{13}+c_{55})u_{3,13} = \rho\ddot{u}_1, \tag{7a}$$
$$c_{66}u_{2,11} + c_{44}u_{2,33} + c_{22}u_{2,22} + (c_{12}+c_{66})u_{1,12} + (c_{23}+c_{44})u_{3,23} = \rho\ddot{u}_2, \tag{7b}$$
$$c_{55}u_{3,11} + c_{44}u_{3,22} + c_{33}u_{3,33} + (c_{13}+c_{55})u_{1,13} + (c_{23}+c_{44})u_{2,23} = \rho\ddot{u}_3. \tag{7c}$$

Waves in unbounded media

Christoffel equations are obtained plugged into the equilibrium equations (7) travelling wave solutions in the form

$$u_i(x_1, x_2, x_3, t) = A_i \exp\left[\imath(k_1 x_1 + k_2 x_2 + k_3 x_3 - \omega t)\right], \tag{8}$$

where $\boldsymbol{A} = [A_i]$ is the polarization vector, $\boldsymbol{k} = [k_i]$ the wave vector, ω the wave frequency and $\imath$ the imaginary unit, i.e. $\imath^2 = -1$. Since we restrict attention to waves propagating in the sagittal plane (x_1, x_2), we have $k_3 = 0$ and no dependence on x_3 (i.e. plane strain). We introduce the ratio $\Lambda = k_2/k_1$, which corresponds to the tangent of the angle of wave propagation to the x_1-axis.

The general solution of the Rayleigh-Lamb dispersion problem may be constructed from a superposition of simple waves, named *partial waves* [4, 17]. Partial waves travel along the plate (along x_1) with the same wavenumber $k_1 = k > 0$, while bouncing back and forth at the plate boundaries. Their interaction is generally induced by the boundary conditions and determine the dispersion pattern. Here, $v = \omega/k$ is the phase velocity along x_1.

The determination of the wave vector (eigenvalues) for the Christoffel equations leads to a sixth degree real-coefficient polynomial equation in λ, which may be factored into the product of a second degree polynomial, governing SH waves for which $\boldsymbol{A} = [0, 0, 1]$, with a fourth degree polynomial, governing partial waves polarized in the sagittal plane, i.e. $\boldsymbol{A} = [A_1, A_2, 0]$. Indeed, the corresponding eigenvectors correspond to the wave polarization.

In order to determine the wave vectors we introduce the dimensionless space and time co-ordinates

$$\{\xi_1, \xi_2, \tau\} = \{h^{-1}x_1, h^{-1}x_2, T^{-1}t\}, \tag{9}$$

having let the reference time T in terms of the body shear wave speed c_{SV}

$$T = \frac{h}{c_{SV}}.$$

In this framework, we define the dimensionless velocities

$$V_1 = c_1/c_{SV}, \quad V_2 = c_2/c_{SV}, \quad V_5 = c_{SH}/c_{SV}, \quad V_c = c_c/c_{SV} < V_1.$$

From now on, with a slight abuse of notation, a subscript comma indicates partial differentiation with respect to the relevant dimensionless variables, i.e. $u_{3,1} = \partial u_3/\partial \xi_1$. Besides, for the sake of compactness, we may sometimes drop the explicit indication of functional dependence, e.g. we may write u_i instead of $u_i(\xi_1, \xi_2, \tau)$. The equilibrium equations for plane motions (7) become (cfr.[5])

$$\frac{c_{11}}{c_{66}} u_{1,11} + u_{1,22} + \left(\frac{c_{12}}{c_{66}} + 1\right) u_{2,12} = u_{1,\tau\tau} \,, \tag{10a}$$

$$u_{2,11} + \frac{c_{22}}{c_{66}} u_{2,22} + \left(\frac{c_{12}}{c_{66}} + 1\right) u_{1,12} = u_{2,\tau\tau} \,, \tag{10b}$$

while antiplane motion is governed by

$$\frac{c_{55}}{c_{66}} u_{3,11} + \frac{c_{44}}{c_{66}} u_{3,22} = u_{3,\tau\tau}. \tag{11}$$

We shall look for solutions in the form of plane harmonic waves

$$u_i(\xi_1, \xi_2, \tau) = U_i(\xi_2) \exp \imath(K\xi_1 - \Omega\tau), \quad i \in \{1, 2, 3\},$$

where $K = k_1 h$ and $\Omega = \omega T > 0$ are the dimensionless wavenumber and angular frequency. With these definitions, $V = \Omega/K = v/c_{SV}$. Antiplane motions give immediately the characteristic equation for λ_{SH}

$$\lambda_{SH}^2 = \frac{c_{66}}{c_{44}} K^2 \left(V_5^2 - V^2\right), \tag{12}$$

whence we can write the general solution

$$U_3(\xi_2) = a_1 \lambda_{SH}^{-1} \sinh(\lambda_{SH}\xi_2) + a_2 \cosh(\lambda_{SH}\xi_2), \tag{13}$$

where a_1 and a_2 are arbitrary constants and the solution has been written in a form independent of the sign chosen for λ_{SH}.

The equilibrium equations for the in-plane motion (10) may be cast in terms of a single fourth order ODE in either $U_1(\xi_2)$ or $U_2(\xi_2)$, say

$$a_2 U_1''''(\xi_2) + a_1 U_1''(\xi_2) + a_0 U_1(\xi_2) = 0,$$

which lends the bi-quadratic characteristic equation for λ

$$a_2 \lambda^4 - a_1 K^2 \lambda^2 + a_0 K^4 = 0, \tag{14}$$

where (cfr.[12] with $c_{66}V^2 = \rho c_R^2$)

$$
\begin{aligned}
a_2 &= c_{22}c_{66},\\
a_1 &= c_{11}c_{22}\left(1-\frac{V^2}{V_1^2}\right) + c_{66}^2(1-V^2) - (c_{12}+c_{66})^2\\
a_0 &= c_{11}c_{66}\left(1-V^2\right)\left(1-\frac{V^2}{V_1^2}\right).
\end{aligned}
$$

The coefficient a_1 is the generalization to orthorhombic materials of the coefficient B of [17]. Clearly, the sign of λ is immaterial and therefore, without loss of generality, we restrict attention to the pair of solutions of Eq.(14) with positive real part

$$\lambda_{1,2} = K\Lambda_{1,2}, \quad \Re(\Lambda_{1,2}) \geq 0, \tag{15}$$

being

$$\Lambda_{1,2}^2 = \frac{a_1 \mp \sqrt{\Delta}}{2a_2}, \quad \Delta = a_1^2 - 4a_0a_2. \tag{16}$$

With this restriction, a branch cut for the square root is selected. With such definitions, $\Lambda_{1,2} = \Lambda_{1,2}(V^2)$ are functions of the phase velocity squared V^2. Physically, $\Lambda_{1,2}$ represent the ratio between longitudinal and transversal wavenumbers, i.e. $\tan\beta$, where β is the angle of wave propagation to the x-axis. In particular, whenever $\Lambda_{1,2} = 0$ an infinite plane wave-front propagating indefinitely is possible, that is a bulk wave. In the isotropic case, we have that the discriminant $\Delta = \mu^2(\lambda+\mu)^2K^2V^2$ is always positive and, as expected, $\Lambda_{1,2}(0) = 1$ for standing waves propagate equally in either direction. When $\Delta < 0$, $\Lambda_{1,2}^2$ becomes a complex conjugated pair describing evanescent waves. The expressions for $\lambda_{1,2}$ represent a generalization to orthothropic materials of Eq.(17) of [17]. Similarly to there, the smallest solution (in terms of absolute value) of (16) corresponds to quasi-longitudinal waves (QP), while the largest gives quasi-shear waves (QSV)*. We observe that Eq.(14) is also the secular equation for the attenuation index of Rayleigh waves, see [15, Eq.(10)] and [16, Eq.(5.54)], with $a_1/a_2 = S$ and $a_0/a_2 = P$. For large values of V we get

$$\Lambda_1 = -V^2, \quad \Lambda_2 = -V^2/V_2^2. \tag{17}$$

*In [17] reference is made to the minus and to the plus solutions, which however correspond to the smallest and to the largest only inasmuch as $a_1 > 0$.

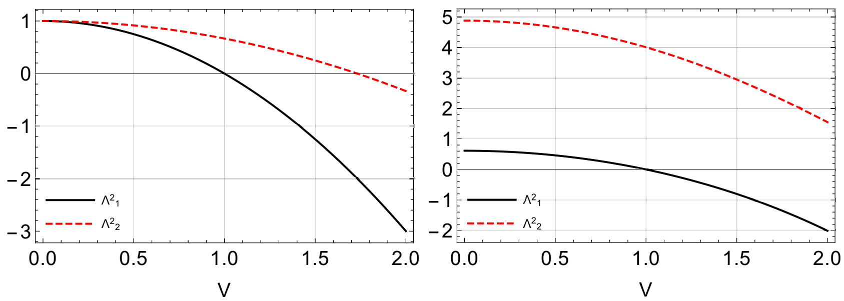

(a) Isotropic material **(b)** Carbon epoxy composite

Figure 2. $\Lambda_{1,2}$ vs. V

It is expedient to introduce the auxiliary quantity

$$V_*^2 = \left(1 + V_2^{-2}\right)^{-1}\left(V_c^2 - 2\frac{c_{12}}{c_{22}}\right), \tag{18}$$

such that the sign of a_1 may be easily determined from

$$a_1 = c_{66}^2\left(1 + V_2^2\right)\left(V_*^2 - V^2\right).$$

We observe that, in general, V_*^2 may be positive, negative or zero. Assuming the condition

$$c_{66} \le \sqrt{c_{11}c_{22}} - c_{12}, \tag{19}$$

warrants that $V_*^2 \ge 0$. Besides, if $c_{12} \ge 0$, we have $0 < V_*^2 < V_c^2 < V_1^2$ and $a_1 \gtreqless 0$ provided that $V^2 \lesseqgtr V_*^2$. In the isotropic case, the inequality (19) is strickly satisfied and we have

$$V_*^2 = 2\left(1 - \frac{1}{1+V_1^2}\right). \tag{20}$$

We observe that, according to Eq.(20), we have $1 < V_* < V_1$. With the usual restriction on the Lamé constants, it is further seen that $2\sqrt{2/7} < V_* < \sqrt{2}$. Hereinafter, to fix ideas, we shall assume that

$$1 < V_* < V_c < V_1 \tag{21}$$

holds also in the orthorhombic case, which is usually the case for real orthorhombic materials.

Speed	Steel	Carbon-epoxy
V_*	1.24	1.92
V_c	1.69	2.45
V_1	1.87	2.48
V_2	1.87	1.43
V_R	0.93	0.96

Table 1. Dimensionless wave speeds for steel (22) and carbon-epoxy (23)

In the following, when giving numerical results, we shall consider steel as a prototype for isotropic materials

$$\lambda = 115 \text{ GPa} \quad \mu = 77 \text{ GPa}, \tag{22}$$

and carbon-epoxy composite for orthorombic materials

$$c_{11} = 55.15 \text{ GPa}, \quad c_{22} = 18.38 \text{ GPa}, \quad c_{66} = 9.00 \text{ GPa}, \quad c_{12} = 4.60 \text{ GPa}. \tag{23}$$

Tab.1 gathers the dimensionless speeds for both materials. Fig.2 shows that $\Lambda_{1,2}^2$ are monotonic decreasing functions of V that are concave downwards, i.e. $\mathrm{d}^2\Lambda_{1,2}/\mathrm{d}V^2 < 0$. They possess the simple zero $\Lambda_1^2(1) = \Lambda_2^2(V_1) = 0$ and, consequently, $V = 1$ and $V = V_1$ are branch points for the square root in $\Lambda_{1,2}$, respectively. It follows that the relevant derivatives $\mathrm{d}\Lambda_1/\mathrm{d}V(1)$ and $\mathrm{d}\Lambda_2/\mathrm{d}V(V_1)$ turn unbounded. Obviously, $\Lambda_{1,2}$ are both real for $V < 1$, respectively purely imaginary and real for $1 < V < V_1$ and both purely imaginary for $V > V_1$. For future purposes, we determine

$$\Lambda_1^2(V_1) = -\left(1 + V_2^{-2}\right)\left(V_1^2 - V_*^2\right). \tag{24}$$

The solution of the equilibrium equations (10) is

$$\begin{bmatrix} U_1(\xi_2) \\ U_2(\xi_2) \end{bmatrix} = \mathbf{G}\boldsymbol{\varphi} \tag{25}$$

where $\boldsymbol{\varphi} = [e_1, e_2, o_1, o_2]$ and

$$\mathbf{G} = \begin{bmatrix} \cosh(\lambda_1\xi_2) & \cosh(\lambda_2\xi_2) & \lambda_1^{-1}\sinh(\lambda_1\xi_2) & \lambda_2^{-1}\sinh(\lambda_2\xi_2) \\ \imath\alpha_1\sinh(\lambda_1\xi_2) & \imath\alpha_2\sinh(\lambda_2\xi_2) & \imath\lambda_1^{-1}\alpha_1\cosh(\lambda_1\xi_2) & \imath\lambda_2^{-1}\alpha_2\cosh(\lambda_2\xi_2) \end{bmatrix}.$$

The vector $\boldsymbol{\varphi}$ will be separated in the first and in the second pair of components, namely $\boldsymbol{\varphi} = [\boldsymbol{\varphi}_e, \boldsymbol{\varphi}_o]$. The matrix $\mathbf{G}$ is arranged thus to show that the displacement is indeed independent on the sign of the lambdas. In Eq.(25), we have let the dimensionless functions of V^2 (cfr.[12, Eq.(17)])

$$\alpha_{1,2}(V) = \frac{c_{66}}{c_{12} + c_{66}} \left(\Lambda_{1,2} + \frac{V^2 - V_1^2}{\Lambda_{1,2}} \right). \tag{26}$$

It is worth noticing that $\alpha_1(V)$ blows up for $V \to 1$, for then $\Lambda_1(V) \to 0$ as $\sqrt{V-1}$. Conversely, as $V \to V_1$, it is $\Lambda_2(V_1) \to 0$ and yet $\alpha_2(V_1) \to 0$, while

$$\alpha_1(V_1) = \left(1 + \frac{c_{12}}{c_{66}}\right)^{-1} \Lambda_1(V_1) \tag{27}$$

is purely imaginary in view of (24) and of the inequalities (21). We observe that the Rayleigh function may be written in a symmetric form in terms of α_i and Λ_i, $i \in \{1, 2\}$, as [12]

$$R(V^2) = \begin{vmatrix} \imath\zeta_{11} & \imath\zeta_{12} \\ -\imath\zeta_{21} & -\imath\zeta_{22} \end{vmatrix} = s_1 - s_2,$$

having let

$$\zeta_{11}(V) = 1 + \frac{c_{22}}{c_{12}}\alpha_1\Lambda_1, \qquad \zeta_{12}(V) = 1 + \frac{c_{22}}{c_{12}}\alpha_2\Lambda_2,$$
$$\zeta_{21}(V) = \imath\left(\Lambda_1 - \alpha_1\right), \qquad \zeta_{22}(V) = \imath\left(\Lambda_2 - \alpha_2\right),$$

and, clearly,

$$s_1 = \zeta_{11}\zeta_{22}, \quad s_2 = \zeta_{12}\zeta_{21}.$$

Therefore, we can determine the Rayleigh wave speed V_R as the single real solution of the equation

$$s_1(V_R) - s_2(V_R) = 0. \tag{28}$$

Partial waves

Rayleigh-Lamb waves emerge from consideration of the plate boundary conditions (BCs). In particular, when Mindlin's BCs are considered, either the micro-chain (MC) conditions,

$$\sigma_{22} = 0 \quad \text{and} \quad u_1 = 0, \tag{29}$$

or the lubricated rigid support (LRS) conditions

$$\sigma_{12} = 0 \quad \text{and} \quad u_2 = 0, \tag{30}$$

Rayleigh-Lamb waves collapse into partial waves. In standard practice, symmetric and antisymmetric (flexural) Rayleigh-Lamb waves are discussed separately: they are obtained splitting the problem in its even and odd part with respect to ξ_2, see [4, 17]. This separation holds also for partial waves. For symmetric LRS and antisymmetric MC we have

$$(\alpha_2\lambda_1 - \alpha_1\lambda_2)\sinh\lambda_1\sinh\lambda_2 = 0,$$

while for symmetric MC and antisymmetric LRS it is

$$(\alpha_2\lambda_1 - \alpha_1\lambda_2)\cosh\lambda_1\cosh\lambda_2 = 0.$$

The first set of solutions satisfying either dispersion relation is

$$\lambda_2 = \imath\tfrac{1}{2}m\pi, \quad m \in \{0, 1, 2, \dots\}, \tag{31}$$

and it corresponds to a family of P modes. Therefore, P modes bounce back and forth at the plate boundaries with an integer number, m, of half wavelengths occurring in between. Accordingly, they appear in the same (opposite) fashion at the plate boundaries, i.e. they are symmetric (antisymmetric), when m is even (odd). Antisymmetric waves repeat periodically every two thickness cycles. In particular, the P mode $m = 0$ describes a plane wave with speed $V = V_1$, i.e. it gives bulk longitudinal waves. Symmetric and antisymmetric P modes possess the eigenforms $\boldsymbol{\phi}_{eP} = (0, 1)$ and $\boldsymbol{\phi}_{oP} = (0, 1)$, respectively. Similarly, the second set of solutions

$$\lambda_1 = \imath\tfrac{1}{2}n\pi, \quad n \in \{0, 1, 2, \dots\}, \tag{32}$$

provides a family of SV modes, which may equally be even or odd according to the parity of n. Symmetric and antisymmetric SV modes possess the eigenforms $\boldsymbol{\phi}_{eSV} = (1, 0)$ and $\boldsymbol{\phi}_{oSV} = (1, 0)$, respectively. In the terminology of [1], partial waves describe the uncoupled-blocked systems and their spectra (31,32) form the *skeleton of the eigenvalues*, wherein the wavenumber K acts as variable parameter.

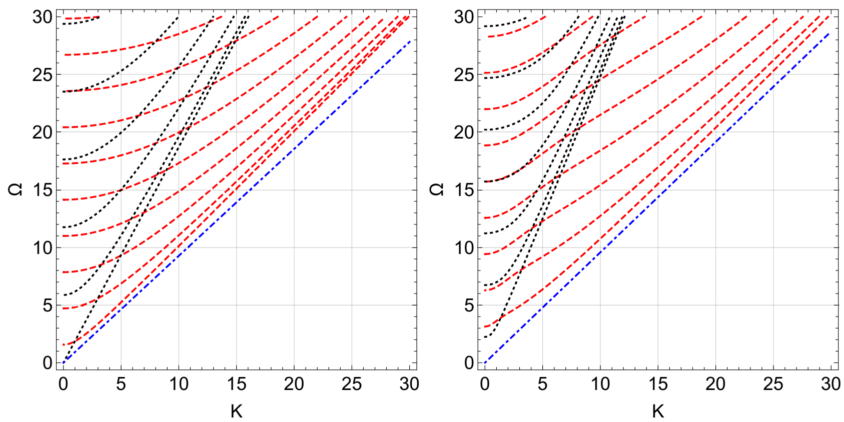

Figure 3. Partial waves for steel: even (odd) P modes (dotted, black) and odd (even) SV modes (dashed, red), respectively left and right panel. The Rayleigh wave line-spectrum is also shown (dash-dotted, blue)

The definition (15) together with Eqs.(31) and (32) show that P and SV modes may be written as a function of K^2 and V^2. The dimensionless group velocity of such partial waves is given by

$$V_{g_{1,2}}(V) = \frac{\mathrm{d}\Omega}{\mathrm{d}K} = V - \frac{\Lambda_{1,2}}{\mathrm{d}\Lambda_{1,2}/\mathrm{d}V}(V) \tag{33}$$

wherein the last term is the reciprocal of the logarithmic derivative. In particular

$$V_{g_1}(1) = 1, \quad V_{g_1}(V_1) = V_1\left(1 - \frac{1 - V_*^2/V_1^2}{1 - \frac{V_2^2(V_1^2-1)}{(1+V_2^2)^2(V_1^2-V_*^2)}}\right) < V_1, \tag{34}$$

and clearly $V_{g_2}(V_1) = V_1$. In the isotropic case, it is $V_{g_1}(V_1) = V_1^{-1}$. In light of the fact that $\Lambda_{1,2}^2$ are decreasing functions of V and observing that Eq.(33) may be rewritten as

$$V_{g_{1,2}}(V) = V - 2\frac{\Lambda_{1,2}^2}{\mathrm{d}\Lambda_{1,2}^2/\mathrm{d}V},$$

it is easily proved that, for $V < 1$, we have $V_g > V$, that is waves move slower than the wave packet as ripples in a pond. However, there are no partial wave branches in that region. For $1 < V < V_1$, there are only SV wave branches describing SV waves moving faster than the wave packet, i.e. $V > V_{g_1}$. Finally, for $V > V_1$, both P and SV waves move faster than the wave packet.

P and SV modes frequency spectra for a steel plate are plotted in Fig.3. It clearly appears that P modes with $m \geq 1$ asymptote bulk longitudinal waves from above and similarly SV modes asymptote bulk SV waves from above. Indeed, writing $\lambda_2 = K\Lambda_2$ and considering the limit $K \to +\infty$ along any curve (31), demands that $\Lambda_2 \to \imath 0$, which in turn requires $V \to V_1^+$, for the product $K\Lambda_2$ to yield a finite purely imaginary number. A similar argument shows that $V \to 1^+$ in the limit $K \to +\infty$ for SV modes (32).

Rayleigh-Lamb waves

For a free plate, we have the BCs

$$\sigma_{22} = \sigma_{12} = \sigma_{32} = 0, \quad \text{at } x_2 = \pm h,$$

that, introducing the constitutive law (6), become

$$\frac{c_{12}}{c_{66}} u_{1,1} + \frac{c_{22}}{c_{66}} u_{2,2} = 0, \quad u_{1,2} + u_{2,1} = 0, \quad \text{and} \quad u_{3,2} = 0, \quad \text{at } \xi_2 = \pm 1. \quad (35)$$

SH waves

As already pointed out, in orthorhombic materials SH waves are decoupled from SV and P waves. Enforcing the last of the BCs (35) on the general solution (13) lends the dispersion relation

$$\sinh(2\lambda_3) = 0,$$

whose solutions are

$$\lambda_3^2 = -p^2\pi^2/4, \quad p = \{1, 2, 3, \dots\}. \quad (36)$$

Besides, we have that $a_1 = 0$ whence $U_3(\xi_2)$ is an even function of ξ_2. The frequency spectrum for SH waves is plotted in Fig.4. It is worth observing that, for large values of K, the spectrum curves tend to the SH bulk wave velocity $V = V_5$.

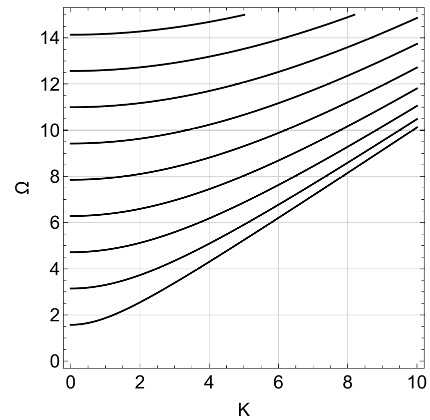

Figure 4. Frequency spectrum (36) for SH waves in a carbon epoxy plate

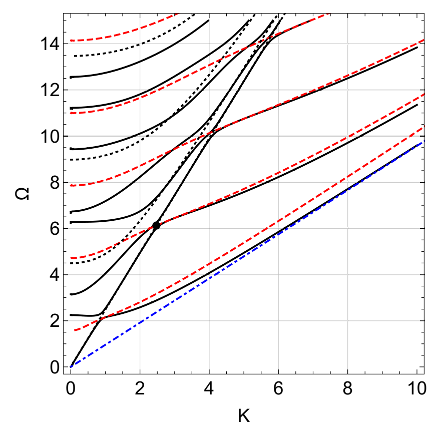

Figure 5. Frequency spectrum for symmetric waves in a free carbon epoxy-resin composite plate superposed onto even P (dotted, black) and odd SV (dashed, red) modes. A veering point (black dot) and the Rayleigh wave line spectrum (dash-dotted, blue) are also presented

Symmetric waves

Consideration of symmetric waves lends the homogeneous algebraic system

$$\mathbf{S}(K,\Omega)\begin{bmatrix} e_1 \\ e_2 \end{bmatrix} = \begin{bmatrix} 0 \\ 0 \end{bmatrix}, \tag{37}$$

where we have let the matrix

$$\mathbf{S}(K,\Omega) = \begin{bmatrix} \zeta_{11}\cosh\lambda_1 & \zeta_{12}\cosh\lambda_2 \\ -\imath\zeta_{21}\sinh\lambda_1 & -\imath\zeta_{22}\sinh\lambda_2 \end{bmatrix}.$$

This matrix may be rewritten in hermitian form

$$\mathbf{S}_h(K,\Omega) = \begin{bmatrix} \imath\zeta_{11}\zeta_{21}\frac{\cosh\lambda_1}{\cosh\lambda_2} & \imath s_2 \\ -\imath s_2 & -\imath\zeta_{12}\zeta_{22}\frac{\sinh\lambda_2}{\sinh\lambda_1} \end{bmatrix}. \tag{38}$$

Demanding that non-trivial solutions of the system (37) exist provides the dispersion relation (cfr.[4, Eq.(8.1.54)])

$$d_s(K^2,\Omega^2) = 0,$$

with

$$d_s(K^2,\Omega^2) = s_1 \coth\lambda_1 - s_2 \coth\lambda_2. \tag{39}$$

The frequency spectrum of a plate made of carbon-epoxy composite is plotted in Fig.5. We observe that odd SV modes are obtained through setting $S_{11} = 0$ and even P modes through putting $S_{22} = 0$, where S_{ij} denotes the (i,j)-element of the matrix $\mathbf{S}$ of Eq.(37).

We observe that the first branch of the spectrum rests in the sector $V < 1$, where $\lambda_{1,2}$ are real numbers, and therefore, for large values of K, we have $\coth\lambda_{1,2} \to 1$ and the solution of (39) tends to the Rayleigh wave speed equation (28). Consequently, for this branch, SV modes cannot act as guiding curves, i.e. the spectrum branches do not follow any of the SV modes (32) (see [17, §4] for a different take on the concept of guiding curve). In contrast, for all the other branches of the Rayleigh-Lamb frequency spectrum, SV modes are guidelines in the short-wave high-frequency (SWHF) regime. This occurs because such branches rest in the sector $1 < V < V_1$ where λ_1 is purely imaginary and λ_2 real; as K grows larger, $\coth\lambda_1$ oscillates wildly unless (32) holds, while $\coth\lambda_2 \to 1$. Then, Eq.(39) is satisfied provided that $s_2 \to 0$, which occurs for $V \to 1^+$. We thus proved that a definite SWHF limit exists provided that the spectrum branches follow odd SV modes and their phase velocity asymptotes the shear bulk wave speed from above. A similar analysis reveals that, in the sector $V > V_1$, P modes act as guiding curves.

We conclude that, when the wavelength becomes very small compared to the plate thickness, only the first spectrum branch is independent of the boundary pair and behaves like only one existed. We can then interpret SV (P) modes as the perturbation of shear (longitudinal) bulk waves which take into account the pair of boundaries.

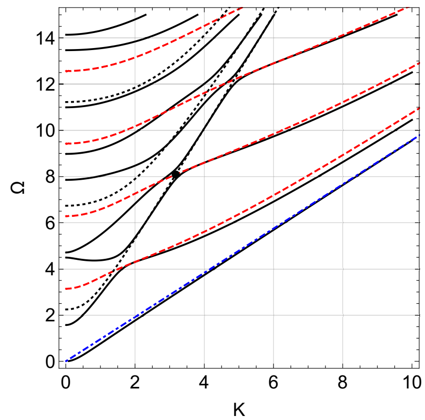

Figure 6. Frequency spectrum for antisymmetric waves (42) in a carbon epoxy-resin composite plate (solid black curves) superposed onto even SV (dashed, red) and odd P (dotted, black) mode spectra. A veering point (black dot) and the Rayleigh wave line spectrum (dash-dotted, blue) are also presented

We further emphasize that the concept of guiding curve is strictly related to the idea of weak coupling in the sense developed in [1]. Indeed, for a weakly coupled system, the spectrum branches quickly collapse onto partial waves outside the close neighbourhood of the veering points.

The long-wave low-frequency (LWLF) approximation of the first symmetric spectrum branch reveals that the system behaviour is equivalent to longitudinal vibrations of a beam-plate with young modulus E_c

$$E_c k^2 = \rho \omega^2.$$

Antisymmetric waves

Consideration of antisymmetric (flexural) waves demands taking the odd part for σ_{yy} and the even part for σ_{xy} in Eqs.(35) and it gives the homogeneous algebraic system

$$\mathbf{A}(K^2, \Omega^2) \begin{bmatrix} o_1 \\ o_2 \end{bmatrix} = \begin{bmatrix} 0 \\ 0 \end{bmatrix}, \tag{40}$$

where

$$\mathbf{A}(K^2, \Omega^2) = \begin{bmatrix} \zeta_{11} \sinh \lambda_1 & \zeta_{12} \sinh \lambda_2 \\ -\imath \zeta_{21} \cosh \lambda_1 & -\imath \zeta_{22} \cosh \lambda_2 \end{bmatrix}.$$

This matrix may be rewritten in hermitian form

$$\mathbf{A}_h(K^2,\Omega^2) = \begin{bmatrix} \imath\zeta_{11}\zeta_{21}\frac{\sinh\lambda_1}{\sinh\lambda_2} & \imath s_2 \\ -\imath s_2 & -\imath\zeta_{12}\zeta_{22}\frac{\cosh\lambda_2}{\cosh\lambda_1} \end{bmatrix}. \tag{41}$$

The corresponding dispersion relation $d_o = 0$ is (cfr.[4, Eq.(8.1.59)])

$$d_o(K^2,\Omega^2) = s_1 \tanh\lambda_1 - s_2 \tanh\lambda_2. \tag{42}$$

The frequency spectrum for flexural waves in a carbon-epoxy plate is shown in Fig.6. We observe that even SV modes are obtained through setting $A_{11} = 0$ and odd P modes through putting $A_{22} = 0$. Once again, the first branch rests in the sector $V < 1$ and therefore it asymptotes Rayleigh waves in the SWHF approximation. Branches in the sector $1 < V < V_1$ are guided by SV modes in the SWHF limit and their phase speed tends to the shear bulk wave speed from above; the argument going as in the symmetric case.

The long-wave low-frequency (LWLF) approximation of the first flexural spectrum branch is given by

$$D_{11}k^4 - 2h\rho\omega^2 = 0, \quad D_{11} = E_c I_{11}, \quad I_{11} = \tfrac{2}{3}h^3,$$

corresponding to flexural vibrations of an orthotropic Kirchhoff beam-plate with flexural rigidity D_{11} and second moment of inertia I_{11}.

Internal veering

In classical veering, as illustrated in [10], the dispersion relation emerges setting to zero the determinant of an hermitian matrix whose off-diagonal terms are small. Indeed, diagonal terms represent the dispersion relation of some mechanically well-defined 1D systems, while off-diagonal terms are expression of the coupling among these. The hermitian nature of the matrix comes from the action-reaction principle. In classical veering, therefore, each system is clearly identifiable at the beginning and likewise are its dispersion modes. Besides, the position of each mechanical system is defined by its own displacement degree of freedom. Veering brings a rotation of the polarization vector from one system to the other. Rayleigh-Lamb dispersion curves exhibit a different form of veering, which we name internal after the observation that it originates from the interaction of SV and P partial waves. In case of internal veering, the definition of the interacting modes is not so straightforward. Also, polarization rotation occurs differently.

Symmetric waves

We now describe the essential features of internal veering with respect to symmetric modes for a free plate. Veering occurs when even P and odd SV modes intersect, that is veering points are located by solving the pair of transcendental equations

$$S_{11} = S_{22} = 0. \tag{43}$$

This amounts to letting in turn $e_2 = 0$ and then $e_1 = 0$. With respect to the terminology developed in [10], this has no correspondence to either the uncoupled blocked system or to the uncoupled disconnected system. Indeed, as already pointed out, P and SV modes emerge from considering Mindlin's mico-chain or lubricated wall boundary conditions. Therefore, the interacting systems share the same kinematical description but differ by the boundary conditions. The off-diagonal entries are coupling terms and they correspond to odd P and even SV modes. In the hermitian writing of Eq.(38), a form of action-reaction principle is preserved.

Let (K_0, Ω_0) define the position of a veering point, i.e. it is a solution of (43). To fix ideas, we consider veering points on the line $\Omega_0 = V_1 K_0$ as in Fig.5, which arise from the interaction between odd SV modes and the first P mode (i.e. bulk longitudinal waves $m = 0$). We observe that this choice appears most unfavourable, for we are right at the branch point for λ_2. K_0 may be simply obtained by solving Eq.(32) with $V = V_1$ (for bulk longitudinal waves we have $\Lambda_2(V_1) = 0$)

$$K_0 \Lambda_1(V_1) = \imath \tfrac{1}{2}(1 + 2n)\pi, \quad n \in \mathbb{N},$$

and making use of Eq.(24), we get

$$K_0^2 = \frac{(\frac{1}{2} + n)^2 \pi^2}{4(1 + V_2^{-2})(V_1^2 - V_*^2)}. \tag{44}$$

We observe that K_0 is real provided that $V_* < V_1$, as we already assumed in (21). Besides, it is easy to see that

$$\mathrm{d}V = \frac{\mathrm{d}\Omega}{K} - \frac{\Omega}{K^2}\mathrm{d}K, \tag{45}$$

and when (K, Ω) lies on a curve $V = const$ we get

$$\mathrm{d}V = 0 \Leftrightarrow V = V_g, \tag{46}$$

that is the phase velocity equals the group velocity. Expanding in Taylor series the matrix $\mathbf{S}_h$ about the veering point is possible, despite the branch point singularity for the square root in $\Lambda_2(V_1)$, because, as already mentioned, the dependence on the lambdas is really through their square, which is the reason by which the sign of the lambdas is immaterial. Indeed we find, at leading order,

$$(\mathbf{S}_{h0} + \mathrm{d}\mathbf{S}_h)\,[K, \Omega, K_0, \Omega_0] = \begin{bmatrix} q_{11}\mathrm{d}K + r_{11}\mathrm{d}\Omega & p_{12} \\ p_{21} & q_{22}\mathrm{d}K + r_{22}\mathrm{d}\Omega \end{bmatrix}, \tag{47}$$

where, after tedious manipulations,

$$r_{11} = -(-1)^n \zeta_{11}(V_1)\zeta_{21}(V_1)\frac{\mathrm{d}\Lambda_1}{\mathrm{d}V}(V_1), \tag{48a}$$

$$r_{22} = -(-1)^n \frac{c_{12}}{c_{12}+c_{66}}\zeta_{12}(V_1)\left(\frac{\mathrm{d}\Lambda_2^2}{\mathrm{d}V}(V_1) - 2\frac{c_{66}}{c_{12}}V_1\right), \tag{48b}$$

and

$$p_{12} = -p_{21} = \imath s_2(V_1). \tag{49}$$

In (48b), the derivative of Λ_2^2 appears that is bounded. Making use of Eqs.(24,27,32), we see that

$$\begin{aligned}
&\zeta_{11}(V_1) = 1 - \frac{c_{66}}{c_{12}}\frac{c_{22}+c_{66}}{c_{12}+c_{66}}(V_1^2 - V_*^2), \\
&\zeta_{12}(V_1) = 1, \\
&\zeta_{21}(V_1) = -\frac{c_{12}}{c_{12}+c_{66}}\sqrt{\left(1+V_2^{-2}\right)(V_1^2 - V_*^2)} = -\frac{c_{12}}{c_{12}+c_{66}}\frac{(\frac{1}{2}+n)\pi}{K_0},
\end{aligned}$$

which are functions of V_1 alone.

In general, $\mathrm{d}K$ and $\mathrm{d}\Omega$ are arbitrary quantities, however, when moving along a SV/P partial wave, we have, respectively,

$$\mathrm{d}(K\Lambda_{1,2}) = 0, \tag{50}$$

whence we get the connection $\mathrm{d}\Omega = V_{g_{1,2}}\mathrm{d}K$ that, substituted into the expansion for $\mathrm{d}S_{11}$ ($\mathrm{d}S_{22}$), yields the result

$$\frac{q_{ii}}{r_{ii}} = -V_{g_i}, \quad i \in \{1, 2\}.$$

We observe that $\mathrm{d}K^2 = 2K\mathrm{d}K$ and $\mathrm{d}\Omega^2 = 2\Omega\mathrm{d}\Omega$, thus $\mathrm{d}\Omega^2/\mathrm{d}K^2 = VV_g$ is the product of the phase and group velocities. Then, recalling that the dispersion relation is a transcendental function of K^2 and Ω^2, we prefer to write (cfr.[10, Eq.(16)])

$$(\mathbf{S}_{h0} + \mathrm{d}\mathbf{S}_h)\left[K^2, \Omega^2, V_1\right] = \begin{bmatrix} \frac{r_{11}}{2\Omega_0}\left(\mathrm{d}\Omega^2 - c_1^2\mathrm{d}K^2\right) & \imath s_2(V_1) \\ -\imath s_2(V_1) & \frac{r_{22}}{2\Omega_0}\left(\mathrm{d}\Omega^2 - c_2^2\mathrm{d}K^2\right) \end{bmatrix}, \quad (51)$$

where, making use of Eq.(46) for c_2,

$$c_1 = \sqrt{V_1 V_{g_1}}, \quad c_2 = \sqrt{V_1 V_{g_2}} = V_1. \quad (52)$$

Consequently, we deduce that, in the neighbourhood of a veering point and within a leading term Taylor approximation, the system behaves like a pair of interacting tout strings, whose wave speeds c_1 and c_2 are the geometric mean of the relevant phase and group velocities. In particular, for all the countable infinite number of veering points on the line $V = V_1$, the tout strings wave speeds are the same and therefore veering repeats itself periodically. In general, we can say that the frequency spectra of the even P and odd SV partial waves define the envelope of the wave speed field for a pair of tout strings whose properties are frequency dependent.

Letting

$$\Delta K = K^2 - K_0^2, \quad \Delta\Omega = \Omega^2 - \Omega_0^2,$$

we write the approximate dispersion relation (cfr.[10, Eq.(14)])

$$\Delta\Omega^2 - (c_1^2 + c_2^2)\Delta K \Delta\Omega + c_1^2 c_2^2 \Delta K^2 - 4\Omega_0^2\eta^2 = 0, \quad (53)$$

with

$$\eta^2 = \frac{s_2(V_1)^2}{r_{11}r_{22}}. \quad (54)$$

The approximation (53) may be obtained directly operating a Taylor expansion of the dispersion relation (39) up to second order terms. The solution of Eq.(53)

provides two branches, named upper and lower,

$$\Delta\Omega = \tfrac{1}{2}(c_1^2 + c_2^2)\Delta K \left(1 \pm \sqrt{1 - 4\frac{c_1^2 c_2^2 - 4\Omega_0^2\eta^2/\Delta K^2}{(c_1^2 + c_2^2)^2}}\right). \qquad (55)$$

It should be emphasized that the string model expansion (51) is consistent inasmuch as $\Omega - \Omega_0$ and $K - K_0$ are small, so that a leading term approximation is meaningful. Assuming $\Omega - \Omega_0 \sim K - K_0 \sim \varepsilon \ll 1$, we have, for the solution set of Eq.(53),

$$4\Omega_0^2\eta^2 \sim 4\Omega_0^2 \left[1 - (c_1^2 + c_2^2)V_1^{-1} + c_1^2 c_2^2 V_1^{-2}\right] \varepsilon,$$

where $\sim$ stands for "same order as". Whence, using (52), we demand

$$\eta^2 \sim \left(V_{g\,1} - 1\right)(V_1 - 1)\,\varepsilon,$$

which is independent of the veering point under consideration, i.e. independent of n. Therefore, here we require η^2 to be small while $4\Omega_0^2\eta^2$ may be, and generally is, large. This approach is at variance with that developed in [10]. As an example, for steel we have $\eta^2 \approx 0.28125$ and for carbon-epoxy $\eta^2 \approx 0.0163$. The smallness of η^2 sets the size of neighbourhood where the tout string approximation is meaningful, regardless of the veering point under scrutiny.

Numerical results

Fig.7 plots the simple approximation (55) for a carbon epoxy composite plate at the veering point corresponding to the SV mode $n = 1$. The same approximation is repeated in Fig.8 for the SV mode $n = 3$ and, as anticipated, the same behaviour is matched. In general, consideration of the leading term alone (string model) appears surprisingly accurate, even in the large, inasmuch as the spectrum branches are well represented (guided) by the corresponding partial waves. For instance, moving along the lower branch in Fig.7, we veer from longitudinal bulk waves (P mode $m = 0$) to the SV mode $n = 1$. In contrast, the upper branch is generally not well described by either partial wave until the close neighbourhood of veering is reached. For this reason, the Taylor expansion method, as here described, is doomed to provide poor accuracy there, no matter how many terms in the expansion. The reason by which the spectrum is not guided by the SV mode on reaching the veering point along the upper branch

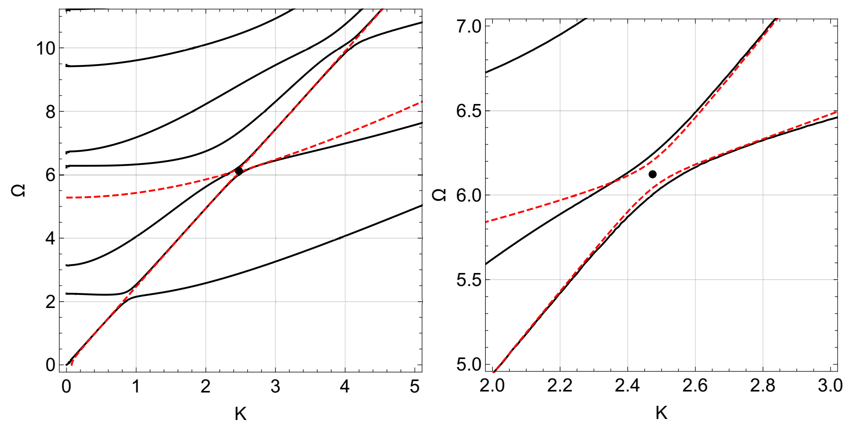

Figure 7. Approximation (55) near the veering point $n = 1$ for a plate made of carbon epoxy composite (dashed, red) superposed onto the frequency spectrum of symmetric waves (solid, black)

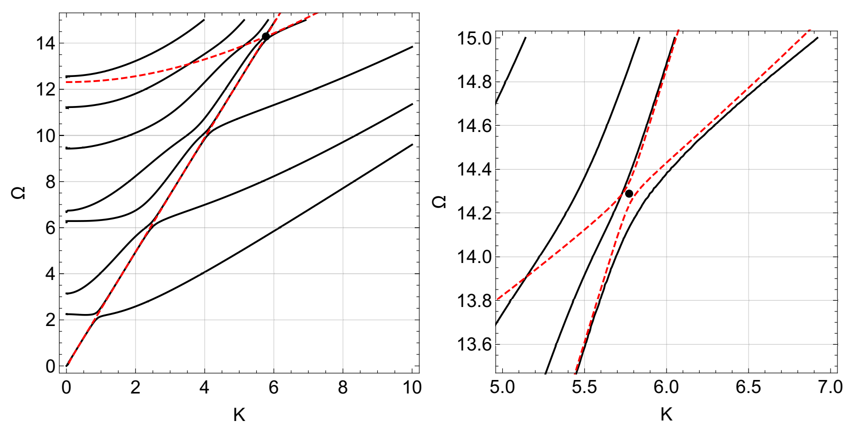

Figure 8. Approximation (55) near the veering point $n = 3$ for a plate made of carbon epoxy composite (dashed, red) superposed onto the frequency spectrum of symmetric waves (solid, black)

may be ascribed to the presence of yet another veering point, so that the two interact (see Fig.5). In fact, moving along the upper branch in Fig.7, we see that the spectrum behaves in between a P and a SV mode until a point $\bar{P}$ is reached where $S_{11} = S_{12} = 0$. Beyond this point, the spectrum approaches the even P mode $m = 0$ and the approximation is excellent again. It should be emphasized that this departure from the guiding curve is not possible in systems of 1D elements, wherein dispersion is bound to a number of dispersion curves.

Conclusions

We analyse Rayleigh-Lamb (RL) modes in an orthorhombic layer with special emphasis on *veering*, that is a coupling phenomenon by which wave branches exchange their role in close proximity to their intersection point (the veering point). Physically, this amounts to destructive wave interference taking place at the veering point (that is a point of no propagation) and constructive interference occurring in its close neighbourhood. Interference occurs in such a way that the ”emerging” wavemodes are swapped compared to the ”incoming” modes. We first recall that RL modes are themselves originating from interference of *partial waves* (here named P and SV modes), which express waves complying with special boundary conditions allowing for no mode conversion. In this sense, partial waves appear ”more fundamental” than RL modes, for it is precisely their combination through the boundary conditions which originates the latter. Indeed, this mechanism is apparent in the frequency spectrum of RL waves, wherein partial waves take up the role of guiding waves, in the sense that they bound the propagation curves. We show here that the same mechanism stands at the ground of veering. Indeed, veering points for symmetric (antisymmetric) RL modes corresponds to intersection points for even P/odd SV (odd P/even SV) partial waves. This situation can be compared with veering in two dimensional systems, wherein eigenmodes pertaining to either mechanical system (considered indipendent or uncoupled) interact by means of the coupling device. In the case of RL modes, asymptotic analysis reveals that interaction occurs in the form of a pair of tout strings whose wave speed are the geometric mean of the relevant wave phase and group velocities. An approximation dispersion relation is obtained whose range of validity depends on the strength of the coupling. Numerical results show that the quality of the approximation is good inasmuch as interaction among neighboring veering points does not occur. Indeed, this interaction weakens the role of partial waves as guiding waves.

Acknowledgements

AN acknowledges financial support from the MSCA RISE EU project 101008140 ”EffectFact”.
BE is grateful for financial support as visiting guest at Modena University.

Declaration of Conflicting Interests

The Authors declare that there is no conflict of interest

References

[1] E Manconi B Mace. Veering and strong coupling effects in structural dynamics. *Journal of Vibrations and Acoustics*, 139(2):021009–021009–10, 2017.

[2] BA Auld. *Acoustic fields and waves in solids*. John Wiley & Sons, 1973.

[3] A Bhaskar. Waveguide modes in elastic rods. *Proceedings of the Royal Society of London. Series A: Mathematical, Physical and Engineering Sciences*, 459(2029):175–194, 2003.

[4] KF Graff. *Wave motion in elastic solids*. Dover Publishing, Inc, New York, 1975.

[5] T Hussain and F Ahmad. Lamb modes with multiple zero-group velocity points in an orthotropic plate. *The Journal of the Acoustical Society of America*, 132(2):641–645, 2012.

[6] RM Jones. *Mechanics of composite materials*, volume 193. Scripta Book Company Washington, DC, 1975.

[7] J Kaplunov and A Nobili. Multi-parametric analysis of strongly inhomogeneous periodic waveguideswith internal cutoff frequencies. *Mathematical Methods in the Applied Sciences*, 40(9):3381–3392, 2017.

[8] JD Kaplunov, LY Kossovitch, and EV Nolde. *Dynamics of thin walled elastic bodies*. Academic Press, 1998.

[9] SV Kuznetsov. Lamb waves in anisotropic plates. *Acoustical Physics*, 60(1):95–103, 2014.

[10] BR Mace and E Manconi. Wave motion and dispersion phenomena: Veering, locking and strong coupling effects. *The Journal of the Acoustical Society of America*, 131(2):1015–1028, 2012.

[11] A Nobili. Asymptotically consistent size-dependent plate models based on the couple-stress theory with micro-inertia. *European Journal of Mechanics-A/Solids*, 89:104316, 2021.

[12] A Nobili and DA Prikazchikov. Explicit formulation for the Rayleigh wave field induced by surface stresses in an orthorhombic half-plane. *European Journal of Mechanics-A/Solids*, 70:86–94, 2018.

[13] A Nobili, E Radi, and C Signorini. A new Rayleigh-like wave in guided propagation of antiplane waves in couple stress materials. *Proceedings of the Royal Society A*, 476(2235):20190822, 2020.

[14] AN Norris. Flexural waves on narrow plates. *The Journal of the Acoustical Society of America*, 113(5):2647–2658, 2003.

[15] D. Royer and E. Dieulesaint. Rayleigh wave velocity and displacement in orthorhombic, tetragonal, hexagonal, and cubic crystals. *The Journal of the Acoustical Society of America*, 76(5):1438–1444, 1984.

[16] D Royer and E Dieulesaint. Elastic waves in solids I: Free and guided propagation. *Springer-Verlag, New York*, 2000.

[17] LP Solie and BA Auld. Elastic waves in free anisotropic plates. *The Journal of the Acoustical Society of America*, 54(1):50–65, 1973.

[18] DJ Thompson, NS Ferguson, JW Yoo, and J Rohlfing. Structural waveguide behaviour of a beam–plate system. *Journal of sound and vibration*, 318(1-2):206–226, 2008.

[19] PE Tovstik. On the asymptotic nature of approximate models of beams, plates, and shells. *Vestnik St. Petersburg University: Mathematics*, 40(3):188–192, 2007.

[20] PE Tovstik and TP Tovstik. Generalized Timoshenko-Reissner models for beams and plates, strongly heterogeneous in the thickness direction. *ZAMM-Journal of Applied Mathematics and Mechanics/Zeitschrift für Angewandte Mathematik und Mechanik*, 97(3):296–308, 2017.

[21] MN Zadeh and SV Sorokin. Comparison of waveguide properties of curved versus straight planar elastic layers. *Mechanics Research Communications*, 47:61–68, 2013.